Learning from RHIC data for the multi-chain model DPMJET-III

ISMD Krakow Sept. 6-11 2003

F. Bopp
Siegen
R. Engel
Karlsruhe
J. Ranft
Siegen
S. Roesler
CERN

1) DPMJET-III

2) Benchmarks (pre RHIC)

3) some RHIC data

4) DPMJET-III + RHIC data
   - percolation + chain fusion
   - $p_\perp$ distributions
   - Collision scaling → R_{AA}

5) Future
   - jet quenching
   - Au-Au → nucleus
   - elliptic flow

High-energy scattering in DPMJET-III

1) hadron-hadron photon-hadron photon-photon	PHOJET Gribov-Regge, AGK cutting r. (LO) perturbative QCD
2) Interaction of high-energy nuclei	Gribov-Glauber Dual Parton Model > 5 GeV HADRIN + formation zone intranuclear cascade < 5 GeV
3) Hadronization of hadronic strings	Lund model PYTHIA-JETSET
4) Intranuclear cascade interaction of produced hadrons in spectator nuclei	Formation zone intranuclear cascade
5) Fragmentation of excited spectator nuclei evaporation of p, n, d, H^3, He^3, He^4 residual nuclei	Nuclear evaporation Fermi-breakup model fission model γ-deexcitation

Comparison to Data (hadron–hadron)

proton – proton

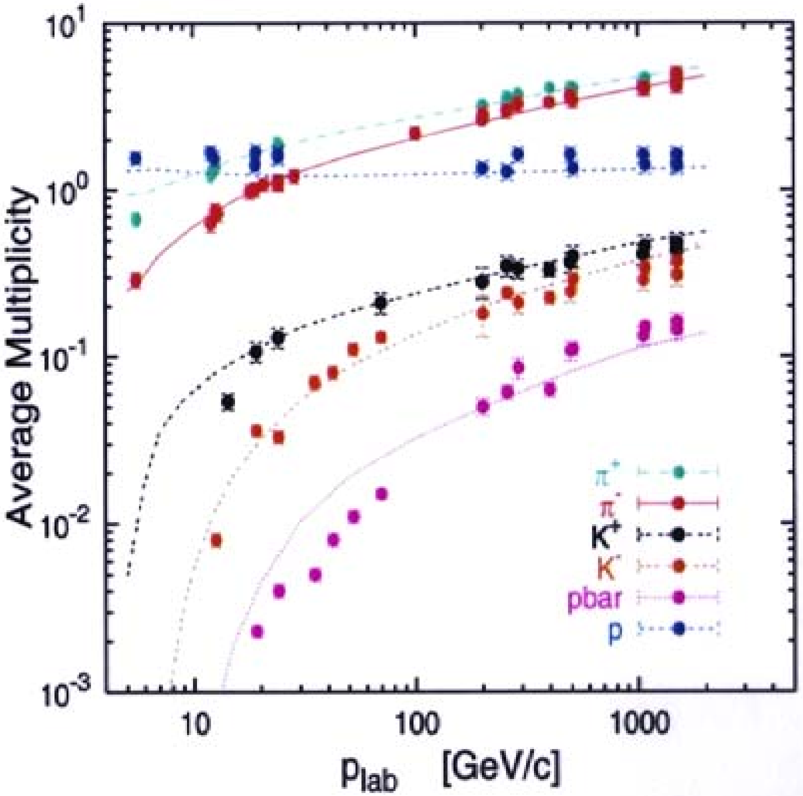

proton – proton, $E_{lab} = 200GeV$

	Exp.	DPMJET–III
charged	7.69 ± 0.06	7.64
neg.	2.85 ± 0.03	2.82
p	1.34 ± 0.15	1.26
n	0.61 ± 0.30	0.66
π^+	3.22 ± 0.12	3.20
π^-	2.62 ± 0.06	2.55
K^+	0.28 ± 0.06	0.30
K^-	0.18 ± 0.05	0.20
Λ	0.096 ± 0.01	0.10
$\bar{\Lambda}$	0.0136 ± 0.004	0.0105

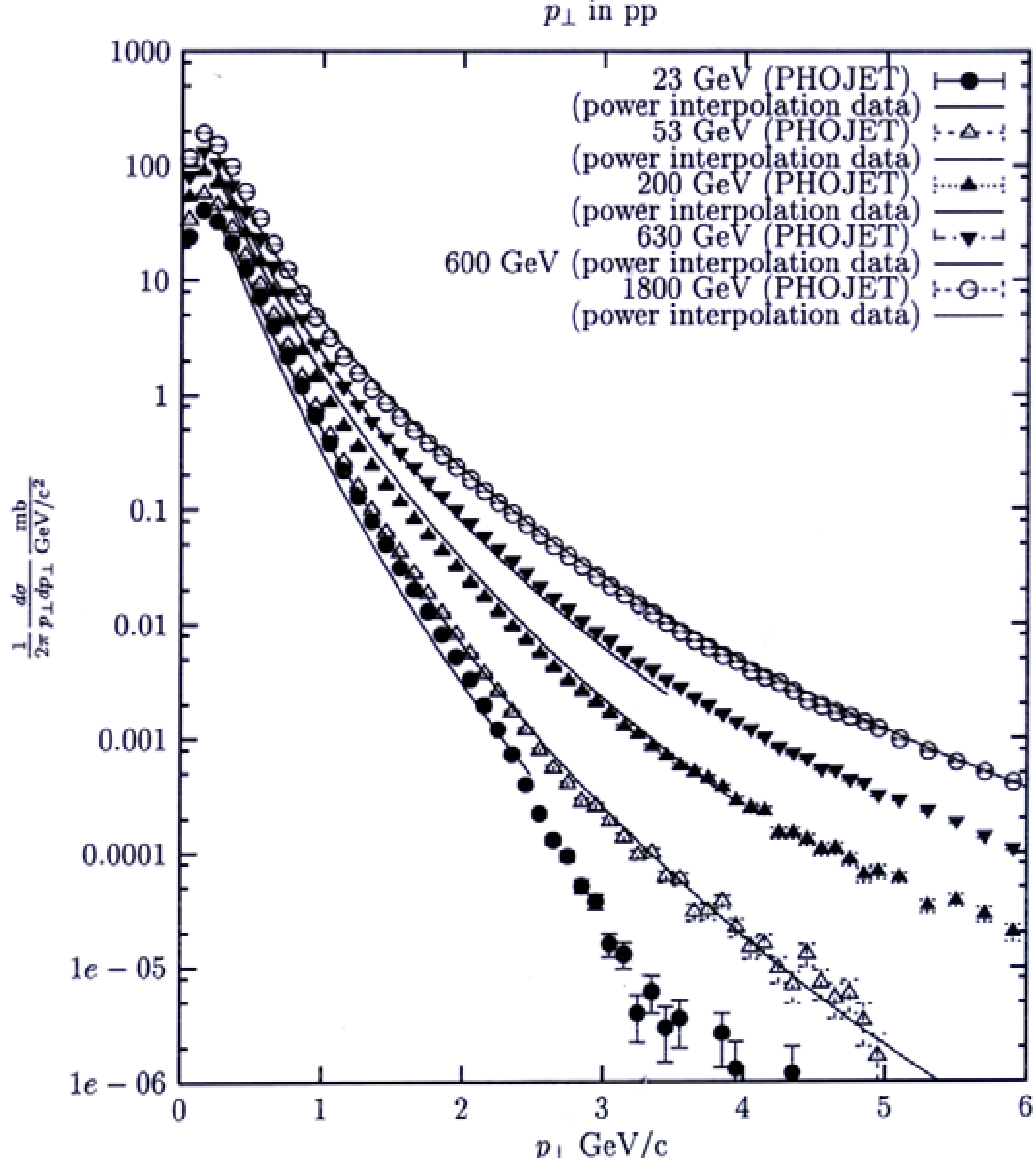

$p_\perp$ in pp
23 GeV (PHOJET)
(power interpolation data)
53 GeV (PHOJET)
(power interpolation data)
200 GeV (PHOJET)
(power interpolation data)
630 GeV (PHOJET)
600 GeV (power interpolation data)
1800 GeV (PHOJET)
(power interpolation data)
$\frac{1}{2\pi}\frac{d\sigma}{p_\perp dp_\perp}\frac{\text{mb}}{\text{GeV}/c^2}$
$p_\perp$ GeV/c

Comparison to Data (nucleus–nucleus)

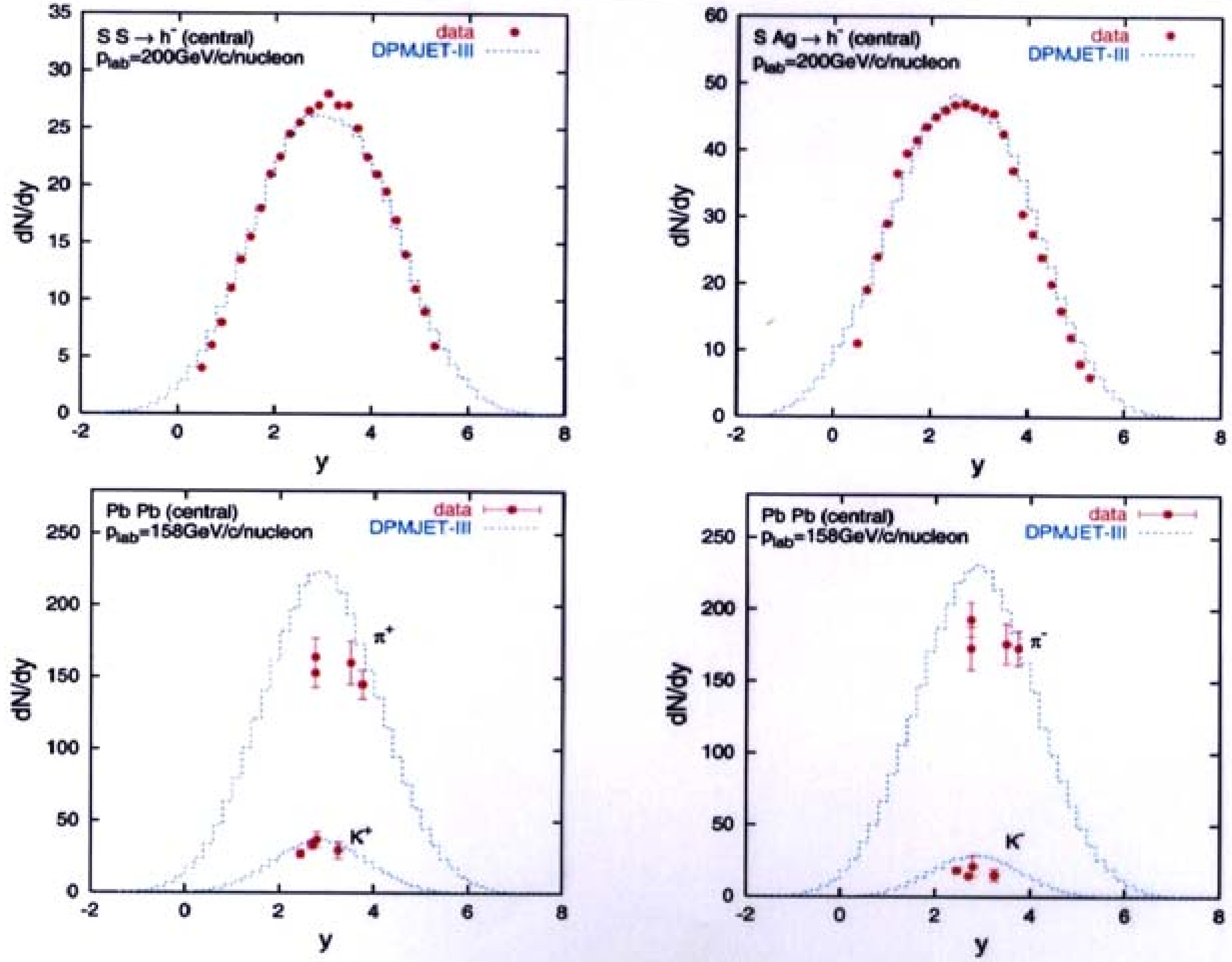

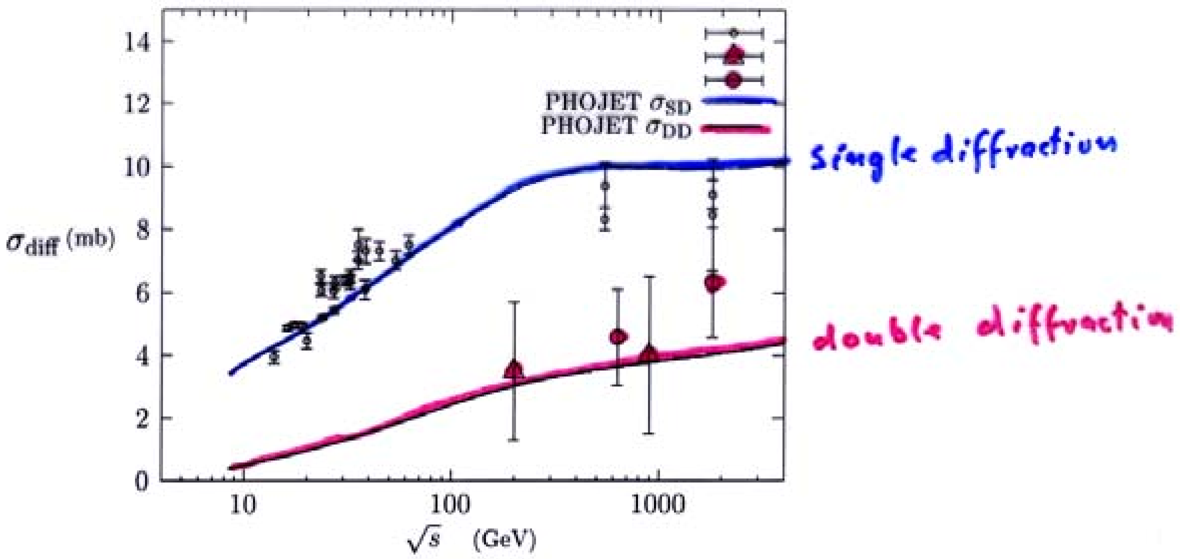

PHOJET σ_{SD}
PHOJET σ_{DD}
σ_{diff} (mb)
$\sqrt{s}$ (GeV)
single diffraction
double diffraction

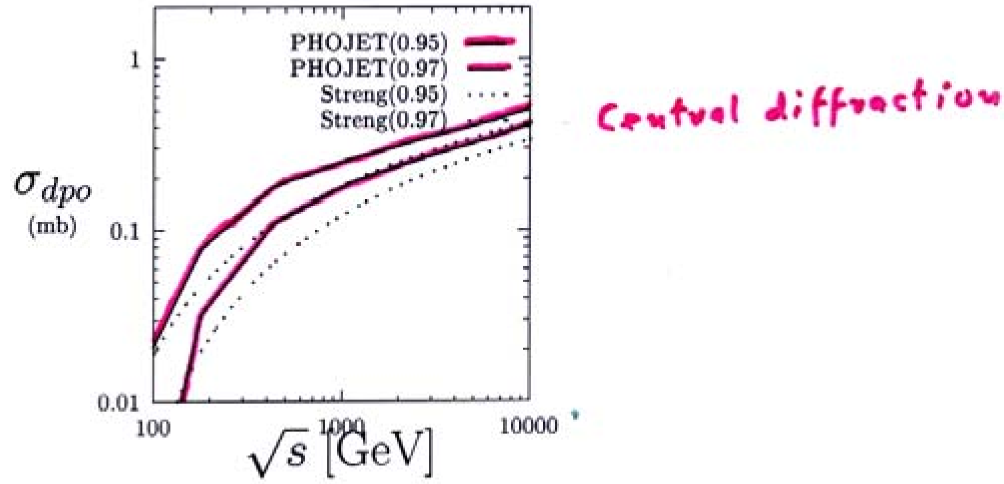

PHOJET(0.95)
PHOJET(0.97)
Streng(0.95)
Streng(0.97)
σ_{dpo} (mb)
$\sqrt{s}$ [GeV]
Central diffraction

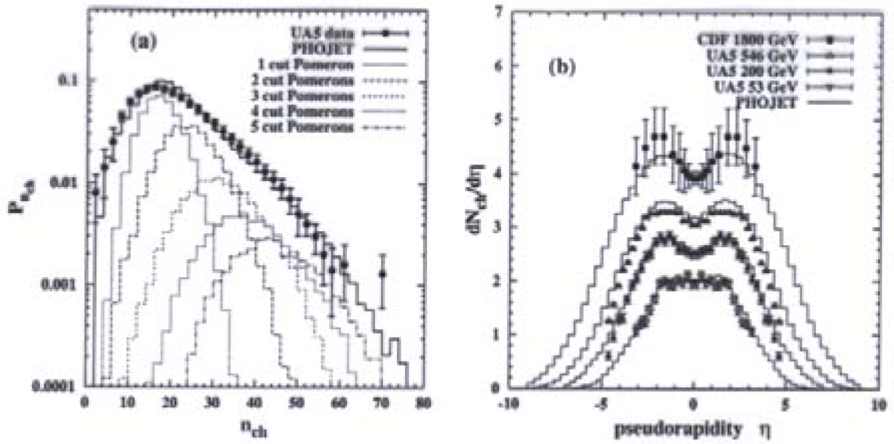

Figure 10. (a) Decomposition of the multiplicity distribution in $p\bar{p}$ collisions according to the number of generated pomeron cuts at $\sqrt{s} = 200$ GeV. (b) Energy-dependence of charged particle pseudorapidity density in $p\bar{p}$ collisions.

event generator[24]) are compared with collider data[22] in Fig. 10.

5 Summary

Regge theory, AGK cutting rules, QCD in the limit of large numbers of colors and flavours, and the geometrical interpretation of high-energy scattering prove very useful in understanding the basic properties of cross sections and multiparticle production. They are some of the tools available today to study soft processes theoretically. Many models combine them to obtain a detailed description of soft processes [5,25,26].

However we are far from being able to reliably calculate predictions for most soft production processes. All approaches or models discussed here have severe shortcomings. For example, Regge theory does not predict transverse momentum-related quantities, and most models implement AGK cutting rules without energy-momentum conservation, to name but a few. Furthermore the rather large number of free parameters limits the predictive power of calculations.

Acknowledgements: This work is supported by U.S. Department of Energy grant DE-FG02 91ER 40626. The author is grateful to L. Frankfurt, T.K. Gaisser, J. Ranft, S. Roesler, T. Stanev, and M. Strikman for many interesting discussions.

RHIC - data

1) Multiplicities and plateau in Au-Au collisions different centralities

2) $p_\perp$ - distributions of identified hadrons

$\pi^0, h^{ch}, \pi^\pm, K^\pm, p, \bar{p}$

3) R_{AA} - ratios

$$R_{AA} = \frac{\frac{d^2N^{A+A}}{dp_\perp d\eta}}{\langle N^{AA}_{bin} \rangle \frac{d^2N^{N+N}}{dp_\perp d\eta}}$$

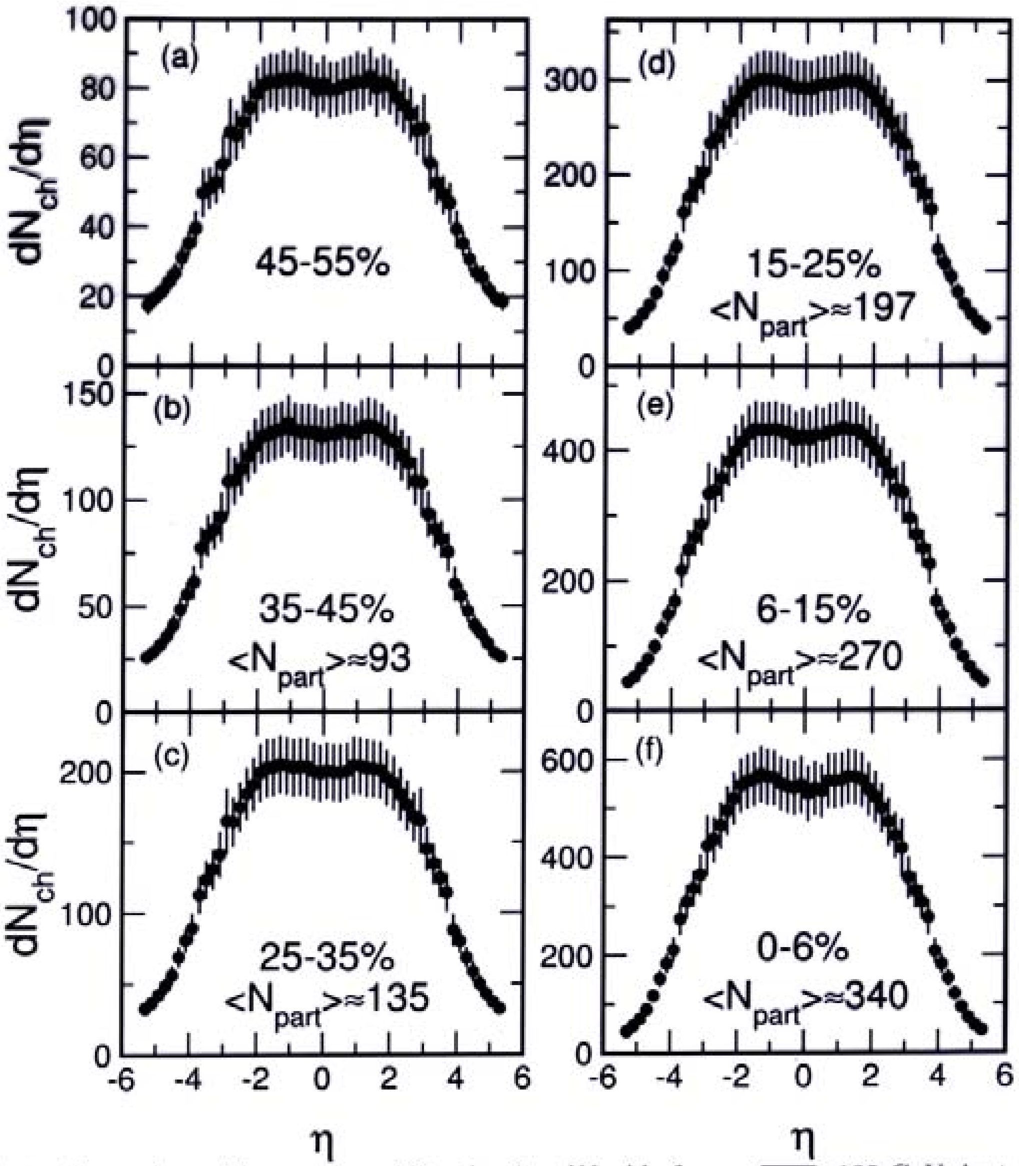

FIG. 1. Charged-particle pseudorapidity density $dN_{ch}/d\eta$ from $\sqrt{s_{NN}}$=130 GeV Au+Au collisions, for different centrality bins, as defined by different fractions of the total observed cross section. The error bars reflect primarily the systematic uncertainties. The average number of participants $< N_{part} >$ for each bin is also indicated. For fractions of the cross section $> 45\%$ the systematic uncertainties in the $< N_{part} >$ determination are still under study and no value is quoted.

PHOBOS 130 GeV

Nucl-ex/0106006

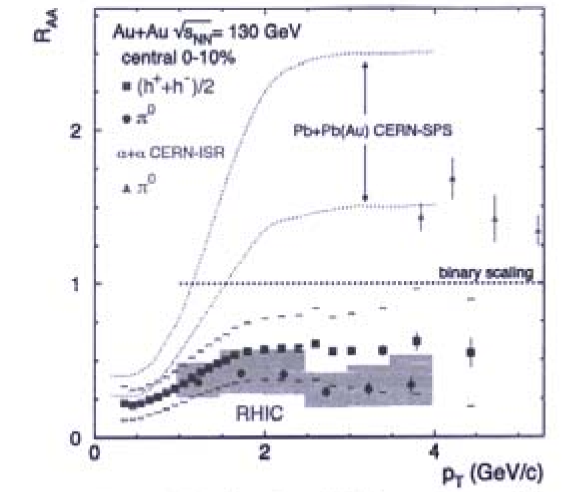

FIG. 2. The ratio R_{AA} for charged hadrons and neutral pions (weighted average of PbSc and PbGl results) in central Au + Au collisions. The error bars indicate the statistical errors on the measurement. The surrounding bands [shaded for π^0's, brackets for $(h^+ + h^-)/2$] are the quadrature sums of (i) the systematic errors on the measurement, (ii) the uncertainty in the $N + N$ reference, and (iii) the uncertainty in $\langle N_{\text{binary}} \rangle$. Also shown are the ratio of inclusive cross sections in $\alpha + \alpha$ compared to $p + p$ at $\sqrt{s_{NN}} = 31$ GeV [18], and spectra from central Pb + Pb, Pb + Au compared to $p + p$ collisions at $\sqrt{s_{NN}} = 17$ GeV [17] shown as a band indicating the range of uncertainty.

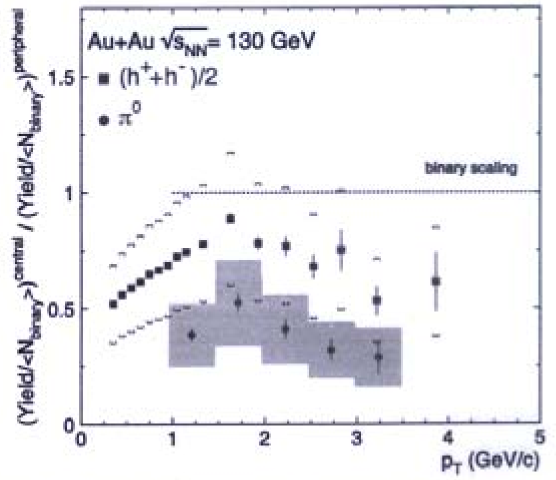

FIG. 3. Ratio of yield per event in central vs peripheral Au + Au collisions, with each divided by $\langle N_{\text{binary}} \rangle$ for that class. For π^0 the weighted average of PbSc and PbGl results is shown. The error bars indicate the statistical errors on the spectra. The surrounding bands [shaded for π^0's, brackets for $(h^+ + h^-)/2$] are the quadrature sums of (i) the parts of the systematic errors on the spectra that do not cancel in the ratio, and (ii) the uncertainty in $\langle N_{\text{binary}} \rangle$ (see Table I).

We can also examine the spectra from central collisions for modifications at high p_T by comparing them to the spectra from peripheral collisions after dividing each by the corresponding values of $\langle N_{\text{binary}} \rangle$. The central-to-peripheral ratio is a useful complement to R_{AA}, since it should be unity in the limit of point-like scaling. Many of the experimental uncertainties are reduced in this ratio (see Table I). Additionally, the uncertainty induced by the $p + p$ interpolation is eliminated, albeit at the expense of incurring that in $\langle N_{\text{binary}} \rangle$ for the peripheral class. We note that there may be effects from the centrality dependence of nuclear shadowing and/or the Cronin effect that would also be present in this comparison.

The central-to-peripheral ratios are plotted in Fig. 3. Like R_{AA} this ratio is below unity at all observed p_T for both charged hadrons and neutral pions, indicating a suppression of the yield per $N + N$ collision in central collisions relative to peripheral. The difference between the two ratios implies that the π/h ratio is smaller in central collisions than in peripheral.

We have presented spectra for charged hadrons and neutral pions measured at 90° from central and peripheral Au + Au collisions in the PHENIX experiment at RHIC. Above $p_T \sim 2$ GeV/c, the spectra from peripheral collisions appear to be consistent (albeit within a substantial systematic error) with a simple, incoherent sum of underlying $N + N$ collisions. The spectra from central collisions, in contrast, are systematically below the scaled $N + N$ expectation, when compared both to data from $p + p$ collisions and to spectra from Au + Au peripheral collisions. The suppression in central collisions is in qualitative agreement with the predictions of energy loss by scattered partons traversing a dense medium. However, other nuclear medium effects should be understood before a quantitative conclusion can be drawn. Measurements in $p + A$ at RHIC can help in this direction.

We thank the staff of the RHIC project, Collider-Accelerator, and Physics Departments at BNL and the staff of PHENIX participating institutions for their vital contributions. We acknowledge support from the Department of Energy and NSF (U.S.A.), Monbu-sho and STA (Japan), RAS, RMAE, and RMS (Russia), BMBF, DAAD, and AvH (Germany), FRN, NFR, and the Wallenberg Foundation (Sweden), MIST and NSERC (Canada), CNPq and FAPESP (Brazil), IN2P3/CNRS (France), DAE and DST (India), LG-YF, KRF, and KOSEF (Korea), and the U.S.-Israel Binational Science Foundation.

*Deceased.

†Not a participating institution.

[1] J. F. Owens *et al.*, Phys. Rev. D **18**, 1501 (1978).

[2] M. Gyulassy and M. Plümer, Phys. Lett. B **243**, 432 (1990); R. Baier *et al.*, Phys. Lett. B **345**, 277 (1995).

[3] X. N. Wang and M. Gyulassy, Phys. Rev. Lett. **68**, 1480 (1992); X. N. Wang, Phys. Rev. C **58**, 2321 (1998).

2) Interpretation of Multiplicities at RHIC

Dias de Deus et al — Phys. Lett. B 491 (2000) 253; " B 494 (2000) 53; hep-ph/0108253

Braun, del Moral, Pajares — hep-ph/0105263

C. Pajares this meeting

→ Multiplicities lower than in conventional multistring models

→ Need for new mechanism lowering multiplicity

Mechanism Nuclear shadowing
<u>Percolation and fusion of strings</u>

Percolation: Braun, Pajares, Ranft J. Mod. Phys A14 (1999) 2689
Braun, Pajares Eur. Phys. J. C16 (2000) 359
" Phys. Rev. Lett. 85 (2001) 4864
del Moral, Pajares Nucl. Phys. B 92 (2001) 95

Result of Percolation:

simplest percolation result

Multiplicity ↘ $\mu_n = \sqrt{n}\,\mu_1$

Average $\langle p_\perp \rangle$ ↗ $\langle p_\perp^2 \rangle_n = \sqrt{n}\,\langle p_\perp^2 \rangle_1$

2.1) Interpretation of $\bar{p}/p$ ratios at RHIC

Evidence for enhanced baryon stopping

Ranft, Engel, Roesler — Proceedings of ICRC 2001, Hamburg

DPMJET-III and RHIC data

$\left.\frac{dN_{ch}}{dy}\right|_{y=0}$ 0-5% centrality

$\sqrt{s}$ [GeV]	DPMJET-III	PHOBOS	BRAHMS	PHENIX
130	968	613±24	553±36	622±41
200	1161	700±27	625±55	

confirm with DPMJET-III

New mechanism needed
to reduce N_{ch}, $\left.\frac{dN_{ch}}{dy}\right|_{y=0}$

→ Introduce percolation and chain fusion into DPMJET-III

4.1 Examples for percolation in DPMJET-III

Join chains for $R_{chain 1 - chain 2} \leq R_0 \approx 0.55\,fm$

1) $q_1 - \bar{q}_2$
   $q_3 - \bar{q}_4$ $\longrightarrow$ $q_1 q_3 - \bar{q}_2 \bar{q}_4$

2) $q_1 - q_2 q_3$
   $q_4 - \bar{q}_2$ $\longrightarrow$ $q_1 q_4 - q_3$

3) $q_3 - q_1 q_2$
   $q_4 - \bar{q}_1$ $\longrightarrow$ $q_4 - q_2 q_5$
   $\bar{q}_3 - q_5$

4) $q_4 - \bar{q}_1$
   $q_5 - \bar{q}_3$ $\longrightarrow$ $q_4 - \bar{q}_3$
   $\bar{q}_5 - q_1$

Result:

1) Number of chains decreases and with this N_{ch}

2) Enhanced B, $\bar{B}$ production

3) Increased $p_\perp$

DPMJET-III with chain percolation

—•—• lines

Brahms

Phenix

Phobos

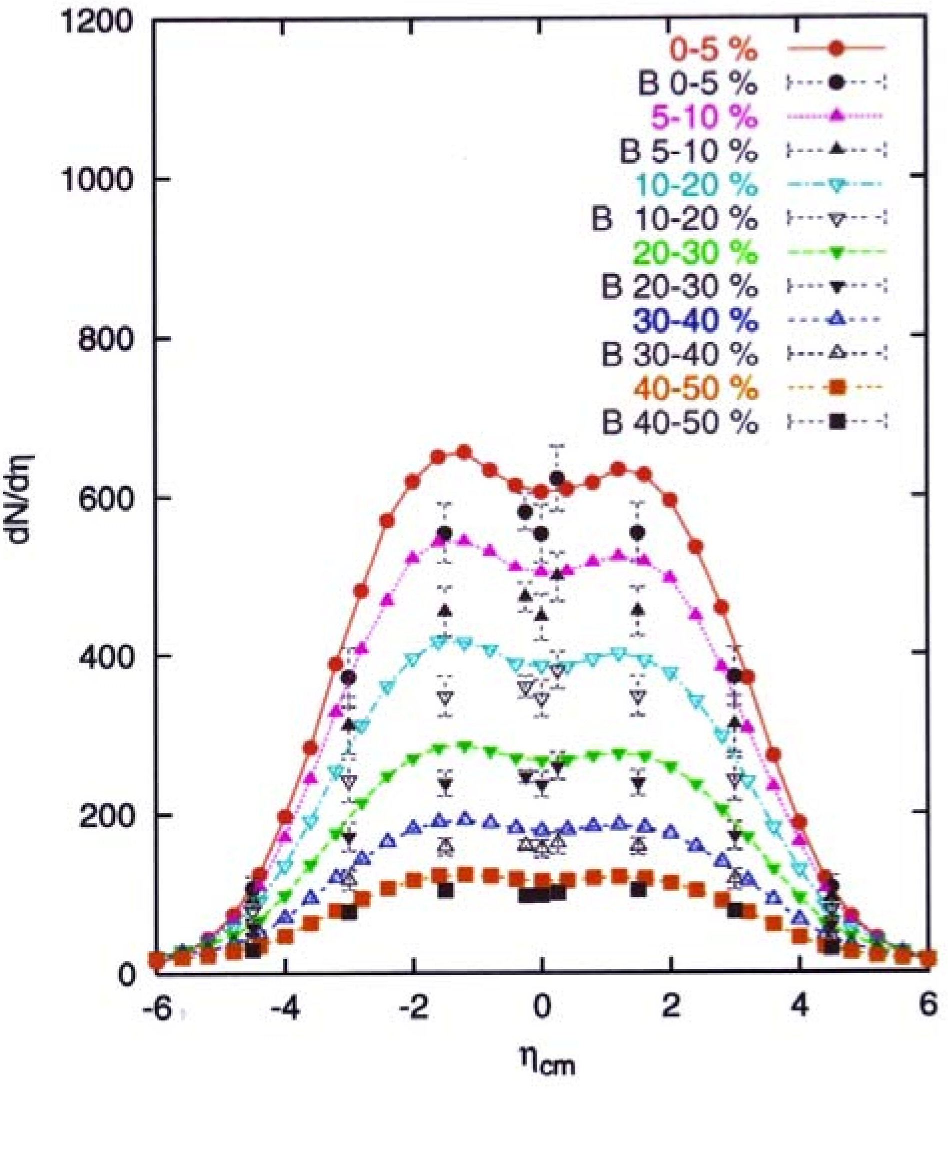

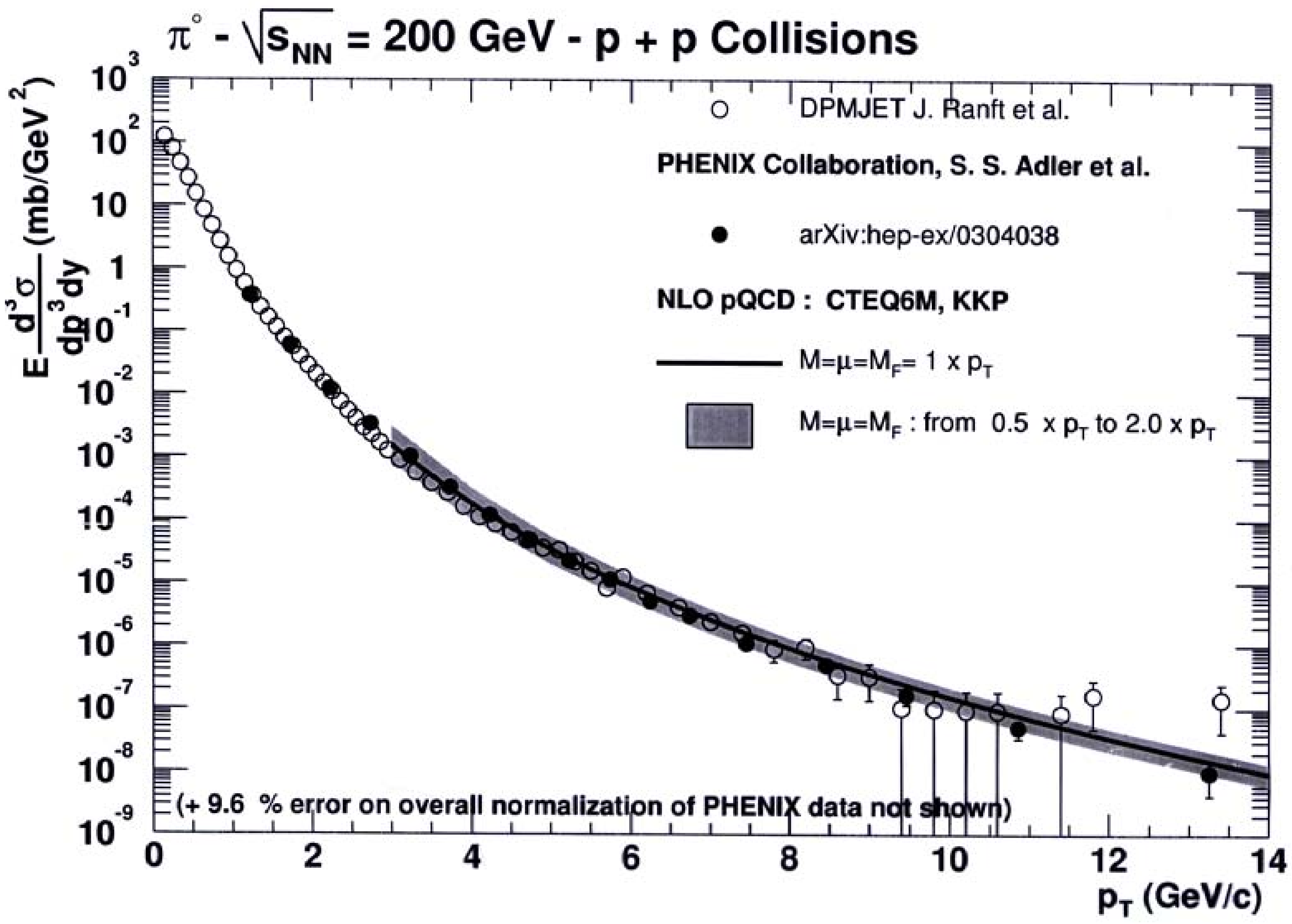

HIC photon group : chair P. Aurenche

Au + Au (130 GeV) → π^-

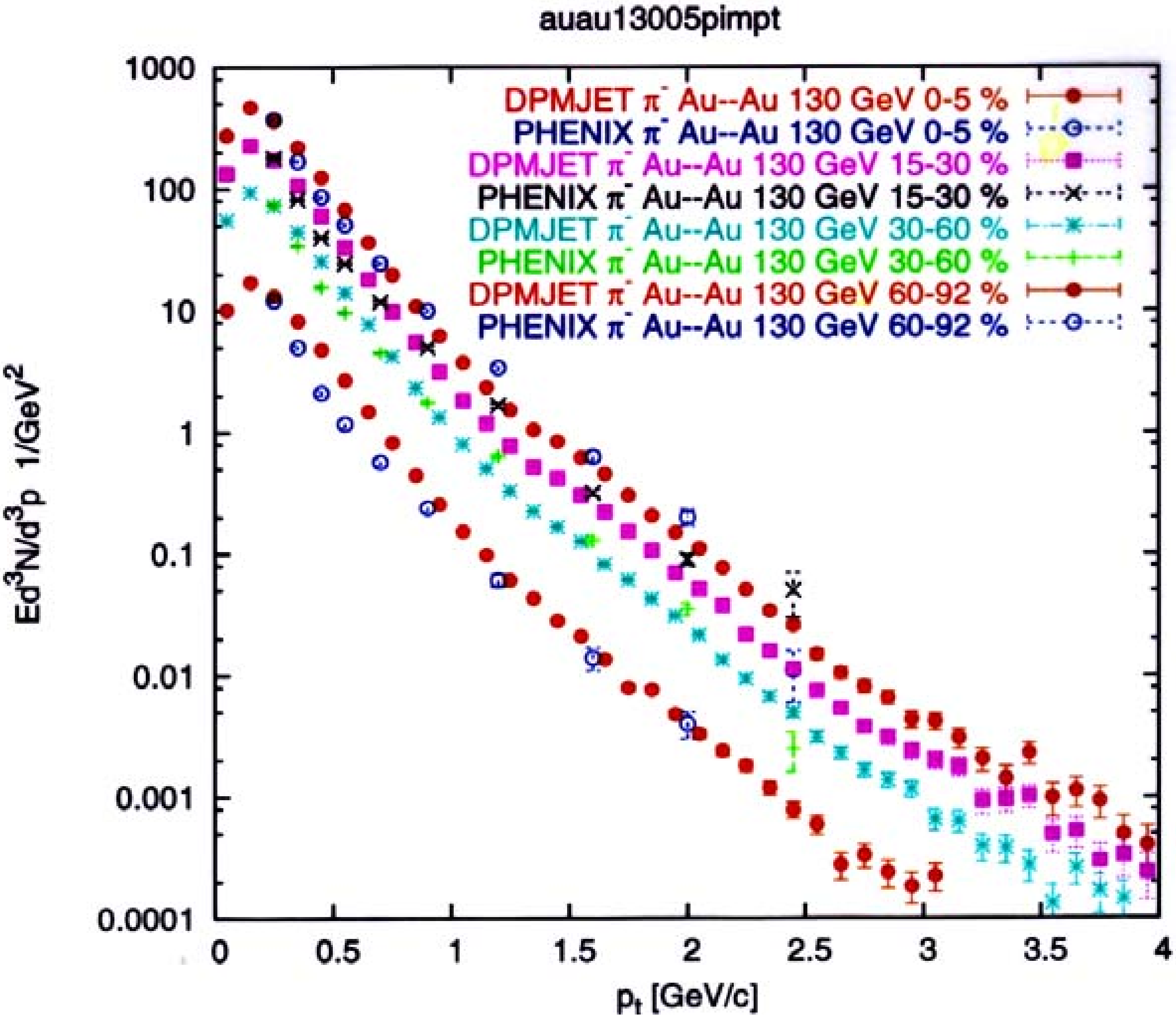

(200 GeV)

Au + Au (0-10%) $\to \pi^0$

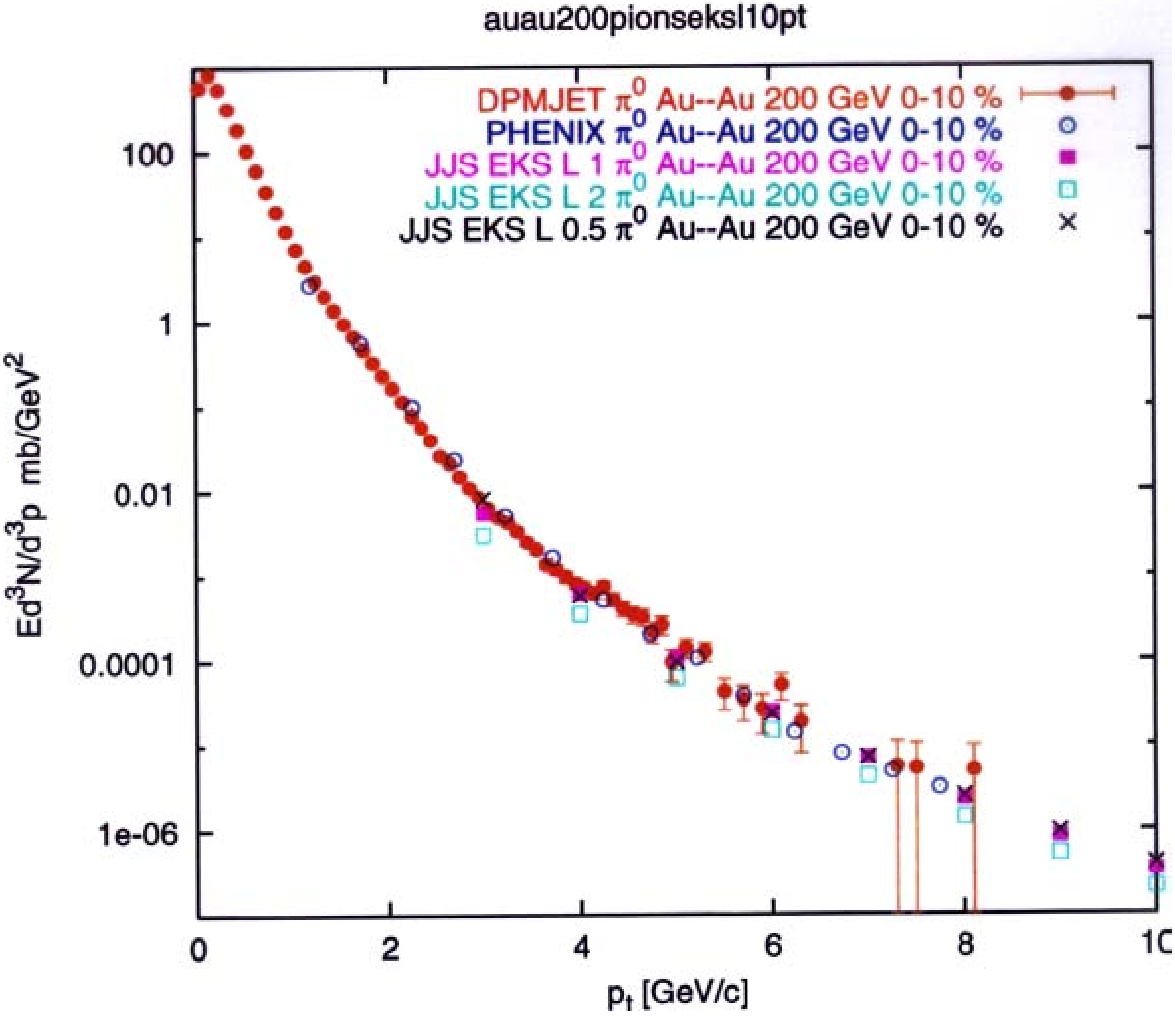

PHENIX data summer 2003

$d + Au \rightarrow \pi^0$

PHENIX: Collision scaling at large p_t

DPMJET: deviations from collision scaling

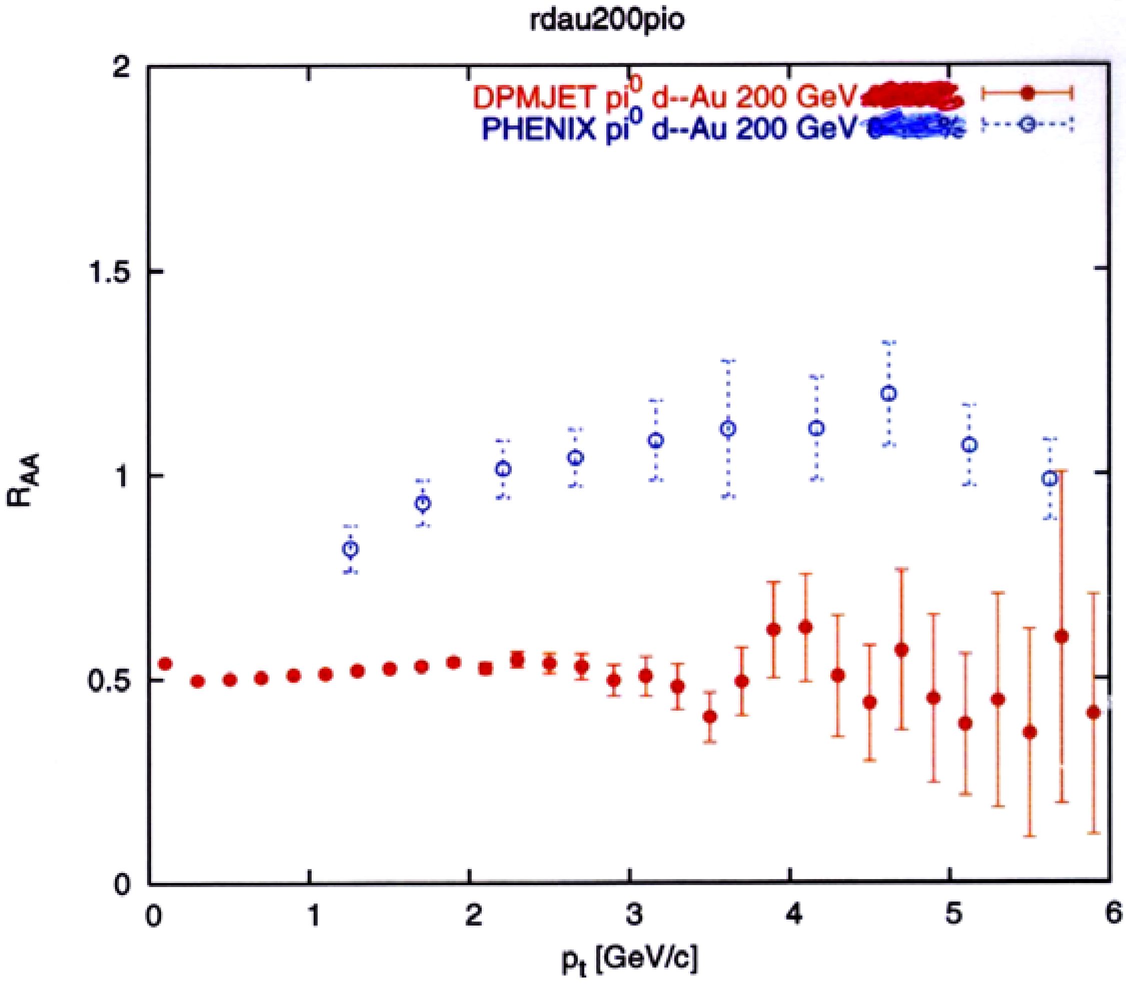

How to obtain collision scaling in DPMJET-III

- No new physics needed
- Glauber cascade

  d-Au (200 GeV) average 4-5 Glauber collisions per projectile

  average 2-3 soft + hard collisions per Glauber collision

  ⟹ 15-25 hard + soft chains per interacting projectile

  conserve energy, momentum, quark flavors
  hard structure functions

Iteration procedure
rejects some soft and hard collisions at low energy in nuclear collisions

⟹ change iteration procedure

d+Au → π⁰ 200 GeV

step 2 changed iteration

nearly collision scaling in DPMJET-III

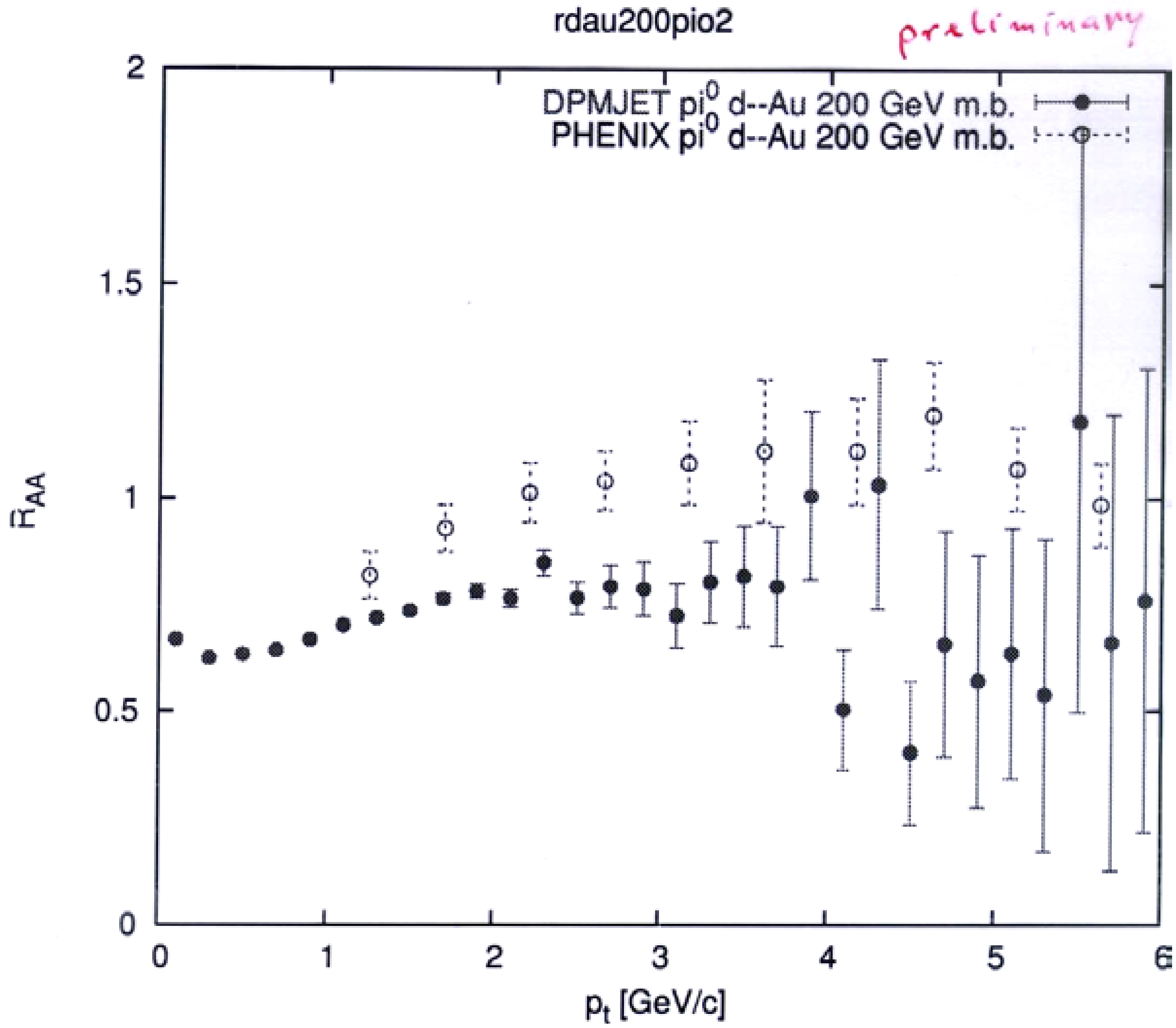

Au-Au (0-10%) (200 GeV) → π⁰

step 1 changed iteration

DPMJET : Deviations from
Collision scaling reduced

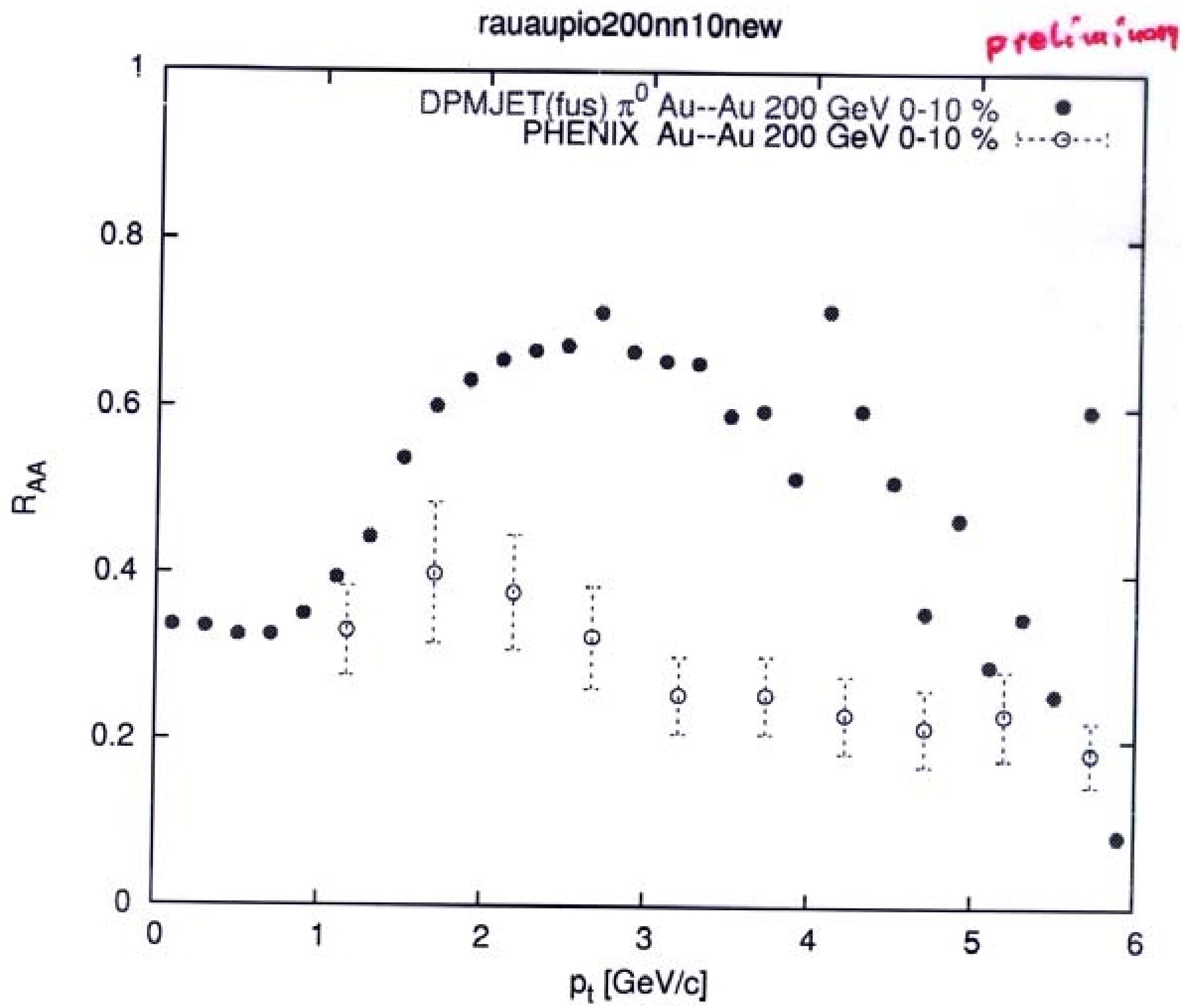

Elliptic flow in RHIC Au-Au Collisions

(often regarded as evidence for hydrodynamic behaviour)

DPMJET-III has some elliptic flow!

calculate v_2 using 2 particle azimuthal correlations

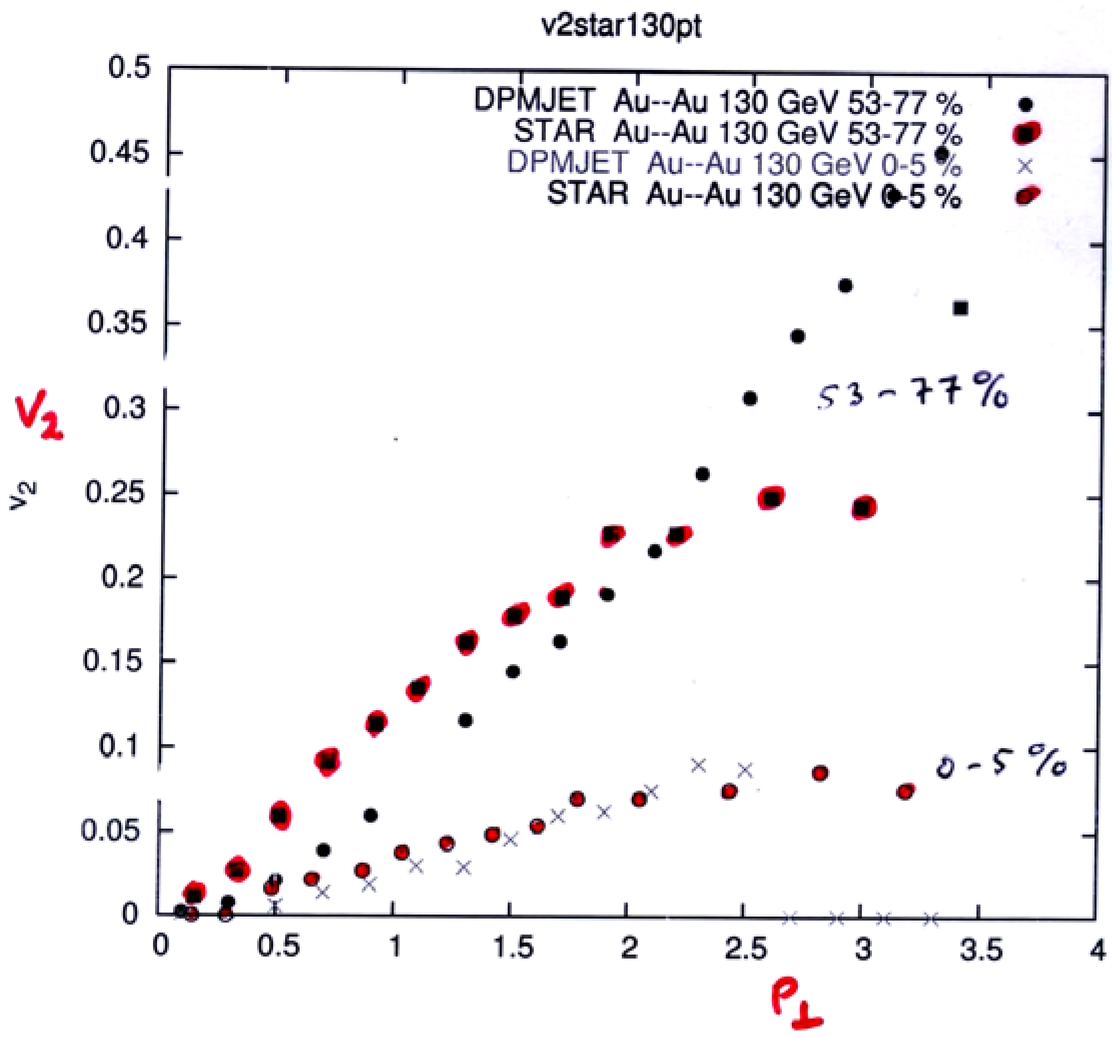

Summary

From RHIC-data we learn

1) Need for percolation and chain fusion

2) Collision scaling in

h - A
d - A collisions

violation of collision scaling in

$Au + Au \rightarrow \pi^0, \pi^\pm$

Continue

jet quenching
$Au + Au \rightarrow$ nucleons
Flow